Journal of Marine Science and Technology

Volume 22 | Issue 4 Article 2

GEOMETRIC SOLUTION IN PROGRESSIVE COLLAPSE ANALYSIS OF HULL GIRDER

Ertekin Bayraktarkatal
Faculty of Naval Architecture and Ocean Engineering, Istanbul Technical University, Maslak, Istanbul, Turkey,
bayrak@itu.edu.tr

Gökhan Tansel Tayyar
Faculty of Naval Architecture and Ocean Engineering, Istanbul Technical University, Maslak, Istanbul, Turkey.

Journal of Marine Science and Technology, Vol. 22, No. 4, pp. 417-423 (2014)
DOI: 10.6119/JMST-013-0513-1

GEOMETRIC SOLUTION IN PROGRESSIVE COLLAPSE ANALYSIS OF HULL GIRDER

Ertekin Bayraktarkatal and Gökhan Tansel Tayyar

Key words: ultimate strength, progressive collapse, curvature, effective width.

ABSTRACT

This paper presents a calculation model for stiffened plates to determine the ultimate strength of ship hull girders from their curvatures using a geometrical approach. The present study employed Smith's method, in which the cross-section is divided into smaller elements consisting of a stiffener(s) and attached plating. The strength of beam-columns and stiffened plates was obtained using an iterative numerical approach. The deflection curve was evaluated using the curvature values directly instead of by solving differential equations. The deflection curve was taken as an assembly of chains of circular arcs. The ultimate strength of the hull girder of a 1/3 scaled frigate model was analyzed using the proposed method through an iterative approach. The present method produced reasonably accurate solutions with low modeling and computational times.

I. INTRODUCTION

A new type of calculation model was presented for stiffened plates to determine the ultimate strength of ship hull girders from the curvatures using a geometrical approach, the curvature-based deflection method [10]. Smith's method, in which the cross-section is divided into smaller elements composed of a stiffener(s) and attached plating, is employed for utilizing the results of the present approach. The shape of the load-shortening relationship was reported to affect the ultimate hull girder strength significantly when Smith's method was applied [16]. Hence, the load-shortening relationship of the element forms the basis of the proposed method.

The load-carrying capacity of a stiffened plate beyond its ultimate strength generally decreases rapidly due to the progress of buckling deformation, which is normally accompanied by localized plastic deformation either in the plate or stiffener. Therefore, it is important to assess the progressive collapse behavior of structural systems, such as hull girder collapse, by examining both the ultimate strength and post-ultimate strength behaviors of stiffened panels [5].

The accuracy of the ultimate strength computations of a ship cross section is closely related to the strength analysis of stiffened plates, which in turn depends on the accuracy of the deflection curve [12, 13]. Therefore, the method proposed in this study focused on mathematical modeling of the deflection curve. In accordance with second order theory, the axial/in-plane stresses rely on accurate modeling of the deflection curve. In addition to using the curvature value in differential equations of the deflection curve, the curvature also represents the deflection geometrically. In this paper, the radius of curvature was used directly in deflection geometry, and the deflection curve was obtained numerically using an iterative method [10, 12, 13]. The deflection curve of the structure was modeled easily using the curvature values, even if the material or geometrical nonlinearities occur [10-13]. Furthermore, the ultimate strength can be obtained using a single numerical procedure, regardless of the structure exhibiting elastic or inelastic behavior [10]. The main motivation of this approach was to reduce the computational and modeling times, as well as to obtain a more precise solution.

The present paper does not include an evaluation of the curvature values from the moment values. In this paper, the effective width calculation method was extended to the curvature based deflection method [12], and an application to column buckling analysis of a perfect beam-column was evaluated by a comparison with the analytical results. In addition, the Dow's Frigate experiment model was assessed and compared with the results reported in the literature.

II. METHOD

Considering the equilibrium of a cross-section of a beam-column or stiffened plate, the internal forces distributed over the cross section were statically equivalent to the external forces. The structure was modeled with a one-dimensional regular curve called the deflection curve, which was generated by the centroids of the cross section of the stiffened plate or beam-column: C moves along its major principal plane normal, as shown in Fig. 1, where s is the curve length of the deflection

Paper submitted 07/25/11; revised 02/22/13; accepted 05/13/13. Author for correspondence: Ertekin Bayraktarkatal (e-mail: bayrak@itu.edu.tr).
Faculty of Naval Architecture and Ocean Engineering, Istanbul Technical University, Maslak, Istanbul, Turkey.

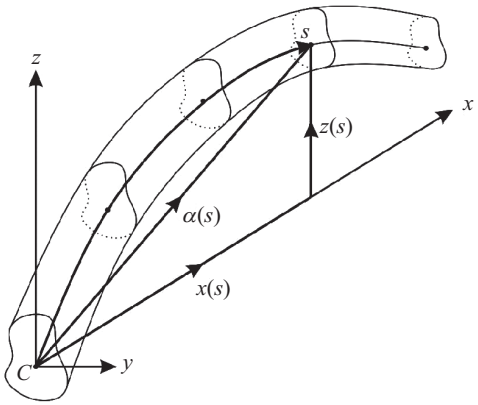

Fig. 1. Deflection curve.

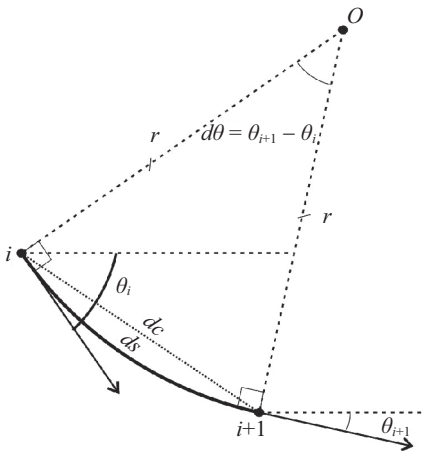

Fig. 2. Curvature.

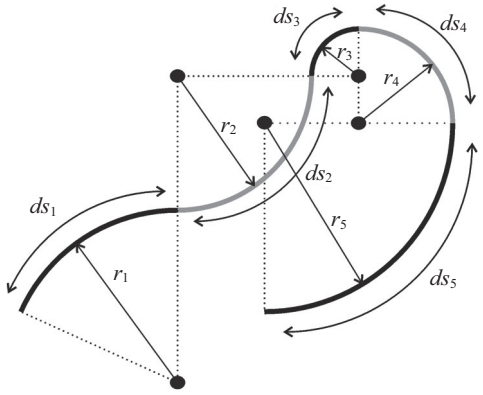

Fig. 3. Curve Modeling [12].

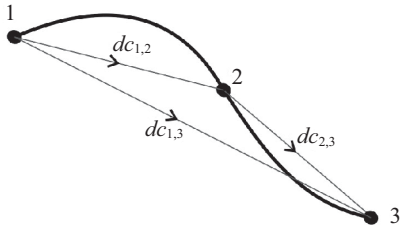

Fig. 4. Displacement vectors of a deflection curve [13].

curve [13]. The deflection curve is an arc length parameterized continuous and differentiable curve that can be defined by the position vector, $\boldsymbol{\alpha}(s) = x(s)\boldsymbol{i} + z(s)\boldsymbol{k}$ [13].

Considering a sufficiently small segment between points i and i+1 on the deflection curve, the length between these points is ds. The tangent angles at points i and i+1 between the x-axis are θ_i and θ_{i+1}, respectively (Fig. 2). By taking the segment, ds, as being sufficiently small, it was assumed that the change in curvature across the segment would be negligible. Therefore, the shape of the segment indicates the arc of a circle with a uniform curvature distribution [12, 13]. This constant curvature also equals the ratio of the difference between the initial and terminal points of the tangent angle of the segment, and $d\theta$ is the segment length, as expressed in Eq. (1), where r represents the radius of curvature or the radius of the circle of the arc (Fig. 2) and K represents the curvature of the segment [14]. The chord length between these points was dc (Fig. 2) [13]. The curvature equation also makes a connection between kinetic and kinematic analysis.

$$1/r = |K| = |d\theta/ds| \tag{1}$$

The curvature of various points on a deflection curve could be obtained using the reaction forces and the material properties of the cross section. In this case, the deflection curve will be composed of arcs. The curve is represented by a sequence of circular arcs within a user-specified tolerance, and the relationship between the circular arcs is established using the proposed method.

1. Deflection Curve Modeling

The radii of the arcs are insufficient for deflection calculations because their centers are unknown. To appoint the position of the center points of the arcs, adjacent arcs are needed to join with G^1 continuity, which has a common unit tangent vector on common points [1]. Consequently, the arcs have the same unit normal vector at a common point of the deflection curve, which means that a line connecting the center of the adjacent osculating arcs always passes through a common point, as shown in Fig. 3 [13]. Therefore, it is possible to determine the position of the adjacent arc from the previous position of the arc, curve length and radius of curvature [10, 12, 13].

The procedure needs to start from the precise point where tangent angle is known. These points can be selected as the origin point of the deflection curve and procedure. A procedure can be developed where the first point slope is predicted and revised iteratively according to the deflections and slopes at the boundaries or supports. If the first point is between the span of the structure, the procedure should progress separately for the left and right side of the first point unless there is symmetry. For simplicity, zero tangent angle points can be selected as clamped edges or symmetry axis.

Fig. 4 shows the total displacement between points 1 and 3,

which is the vectorial summation of the two displacement vectors. Therefore, the general displacement vector between the starting point and any point of the deflection curve can be obtained by a simple vectorial summation of the displacement vector of all previous segments expressed as follows, where ***i*** and ***k*** represent the unit vectors of the *x*-axis and *z*-axis in the rectangular Cartesian coordinate system, respectively [13]:

$$\begin{aligned} \boldsymbol{dc}_{1,i+1} &= \boldsymbol{dc}_{1,2} + \boldsymbol{dc}_{2,3} + \boldsymbol{dc}_{3,4} + \ldots + \boldsymbol{dc}_{i,i+1} \\ &= x_{i+1}\boldsymbol{i} + z_{i+1}\boldsymbol{k} = \boldsymbol{\alpha}_{i+1} \end{aligned} \tag{2}$$

The tangent angle at point *i* on the deflection curve can be expressed as follows:

$$\begin{aligned} \theta_{i+1} &= \theta_1 + \sum_{n=1}^{i-1} K_{n,n+1} ds_{n,n+1} = \theta_i + d\theta_{i,i+1} \\ &= \theta_i + K_{i,i+1} ds_{i,i+1} \end{aligned} \tag{3}$$

where $K_{i,i+1}$ and $ds_{i,i+1}$ represent the curvature value and curve length between point *i* and point *i*+1 on the deflection curve, respectively [13]. The displacement vector from initial point can be expressed as follows:

$$x_{i+1} = x_i + dx_{i,i+1} = x_i + \frac{1}{K_{i,i+1}}\left(\sin\theta_{i+1} - \sin\theta_i\right) \tag{4}$$

$$z_{i+1} = z_i + dz_{i,i+1} = z_i + \frac{1}{K_{i,i+1}}\left(\cos\theta_i - \cos\theta_{i+1}\right) \tag{5}$$

where x_1, z_1 and θ_1 were taken as zero [13]. The same approach can be used inversely to calculate the initial curvatures. Therefore, there is no need to define the initial deflection with a trigonometric series [10].

III. STIFFENED PLATE MEMBERS

When estimating the ultimate strength of a stiffened panel using simplified methods, it is often necessary to accurately determine the post-buckling effective width of a local plate panel. The interaction between the plating and stiffener in the buckling behavior must also be considered carefully [5]. The effective width of the plating between stiffeners was formulated, accounting for the applied compressive loads, initial imperfections and weld induced residual stresses. The effective width of the buckled plating varies with the compressive loads because it is a function of the applied compressive stress [9]. On the other hand, most simplified methods assume that the effective width of plating does not depend on the applied compressive load, and the ultimate effective width of plating is typically constant. An equation characterizing the ultimate limit condition for a stiffened panel showed a much higher degree of nonlinearity than would otherwise be derived by treating the effective width of the plating as a variable [4].

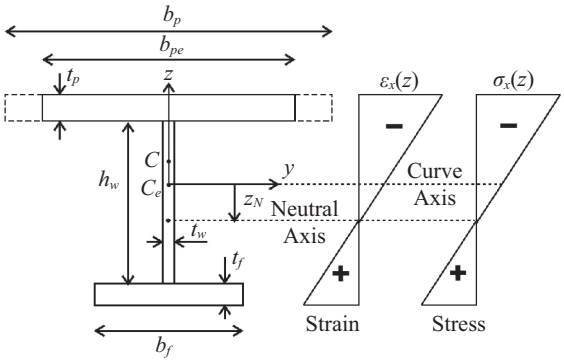

Fig. 5. Stiffened plate cross-section with strain stress distributions.

The initial shape imperfection and welding residual stresses have a significant effect on the buckling collapse behavior of the plate [5]. The concept of the "effective width" has been used for practical design. The pure formula without the empirical formulations of the initial imperfection from von Karman was used for the effective width calculations, as expressed in Eq. (6), where σ_{xmax} and σ_{cr} represent applied maximum edge stress of the structure and critical local plate buckling stress, respectively [3, 7, 15].

$$\rho = \sqrt{\sigma_{cr} \big/ \sigma_{x\max}} \Rightarrow b_e \big/ b = \begin{cases} \rho & \rho \le 1 \\ 1 & \rho > 1 \end{cases} \tag{6}$$

The elastic critical local plate buckling stress can be expressed as follows, where *t* and *b* are thickness and width of the corresponding plate, respectively; *E* is the Young modulus; *v* is the Poisson ratio and *k* is the buckling coefficient.

$$\sigma_{cr} = \frac{k\pi^2 E}{12(1-v^2)}\left(t \big/ b\right)^2 \tag{7}$$

The value of *k* for the attached plating at bottom or deck can be taken as "4" for pure bending [7]. The other type of buckling coefficients for the stiffener web or stiffener flange and local buckling stress are available in [18].

Fig. 5 presents the typical stiffened plate cross section composed of the attached effective plate, web and flange. As a consequence of the effective width calculation, effective dimensions or locations represented by the subscripts, "*e*", can be recalculated.

The stress distribution over the cross section can be defined easily using the curvature values, external loads and material properties. The strain distribution can be achieved using Eq. (8), where z_N represents the shift between the deflection curve axes or between the effective centroids of the cross section, C_e, to the neutral axis (Fig. 5).

$$\varepsilon(z) = K(z_N - z) \tag{8}$$

The stress distribution can be derived using the material properties of the material. The solution for the elastic material can be expressed as follows:

$$\sigma_x(z) = EK(z_N - z) \tag{9}$$

The stress distribution for the elasto-plastic material type can be obtained as follows:

$$\sigma_x(z) = \begin{cases} EK(z_N - z) & \left|K(z_N - z)\right| \le \varepsilon_{yield} \\ \sigma_{yield}\dfrac{K(z_N - z)}{\left|K(z_N - z)\right|} & \left|K(z_N - z)\right| > \varepsilon_{yield} \end{cases} \tag{10}$$

where σ_{yield} and ε_{yield} are the yielding stress and strain of the material, respectively. The internal and external forces need to be in equilibrium over the cross section. Therefore, the stress distribution needs to satisfy Eq. (11), where F_x is the axial normal forces acting on the cross section area, A. The neutral axis position can be defined by Eq. (11). Determination of the curvature value is obtained from Eq. (12) by substituting Eq. (9) or Eq. (10) for elastic type or for elasto plastic type of materials.

$$F_x(z) = \iint_A \sigma_x(z)\,dydz \tag{11}$$

$$M(z) = \iint_A -\sigma_x(z)\,z\,dydz \tag{12}$$

The stiffener plate stress along the longitudinal direction has a distribution that is dependent on the curvature values. The concentrated loads, pressure loads and initial imperfections were considered in the kinetic calculations of the moment curvature. Therefore, there is no need to use the empirical formulations to model the initial imperfection of the deflection curve or add additional formulations to model the external loads.

The stress of the plate was taken as the maximum compressive stress of the attached plate, $\sigma_{xmax\text{-}plate}$ from Eqs. (10) and (11) to obtain the effective width of the stiffener plate in Eq. (13) where $\sigma_{cr\text{-}plate}$ was obtained from Eq. (7). The effect of welding residual stress, σ_R, was included by adding the residual stress directly to the maximum compressive stress of the plate as follows according the studies summarized in reference [7]:

$$\rho_{plate} = \sqrt{\frac{\sigma_{cr-plate}}{\sigma_{xmax-plate} + \sigma_R}} \Rightarrow \frac{b_e}{b} = \begin{cases} \rho & \rho \le 1 \\ 1 & \rho > 1 \end{cases} \tag{13}$$

The collapse modes for stiffened plates reported elsewhere can be classified into six types [7]. Column buckling, yielding or local buckling induced types collapses can be obtained

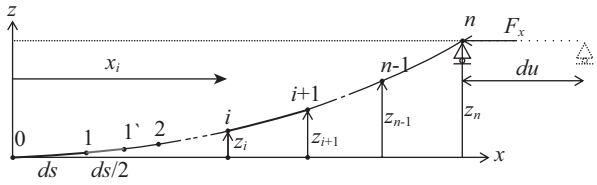

Fig. 6. Displacements of the deflection curve.

easily using the proposed method. Therefore, the application in section IV illustrates the ability of the method to determine column buckling for a perfect beam-column.

On the other hand, the proposed method cannot examine the response to lateral torsional buckling because the method is based on planar displacements of the deflection curve. This one degree of freedom restricts the torsion of the cross section. The method basically models the one dimensional displacements, and it is possible to extend this developing method with two dimensional displacements to determine the torsion behavior.

IV. PROCEDURE

The iteration procedure of the numerical method is based on the assumption that the curvature of a segment is constant and equals the curvature obtained from the midpoint or average moment of the segment. The slope of the first point is zero. Therefore, a symmetrical deflection is expected for the segments of the left and right sides of the start point. The mean moment of the start point can be accepted instead of the midpoint moment value of the first segment. The midpoint coordinates of the following segment were evaluated using the previous segment curvature by assuming that the curvature does not change from the start point of the segment to the midpoint of the following segment. Fig. 6 presents the notations, x and z values are the distance from reference point. The iteration only needs to be performed from the left or right sides of the starting point.

The procedure for the load-shortening calculations is summarized as follows [12]:

1. Define 2n, total number of the segments,
2. Calculate dL, shortening of the structure due to compressive axial load,
3. Calculate segment length; $ds = (L_0 - dL)/(2n)$,
4. Predict du, total horizontal shortening of the boundaries and predict $\delta_{\max}$, maximum deflection; set $x_n = L_0 - du$ and, $z_n = \delta_{\max}$,
5. Set; $i = 0$, $x_i = 0$, $z_i = 0$, $dL = 0$, $\theta_i = 0$,
6. Obtain the average internal forces for the segment i,
7. Calculate dl_i, shortening of the segment i due to the average normal force, and set $dL = dL + dl_i$
8. Calculate $r_{i,i+1}$, radius of curvature value due to internal forces using Eqs. (11) and (12). Consider the initial curvature values if available,

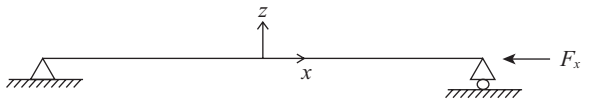

Fig. 7. Euler-column.

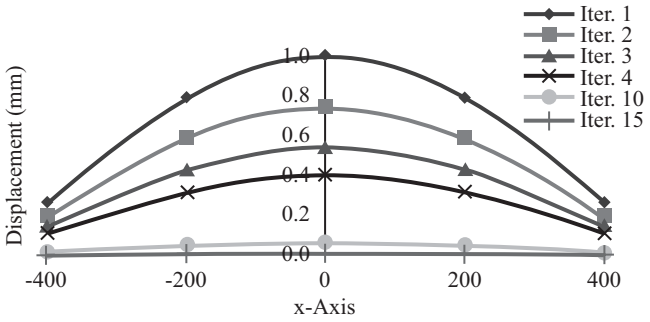

Fig. 8. Deflection curve against the iterations for a 3000 N axial load.

9. Obtain the location of point *i*+1 using Eqs. (4) and (5) with the *ds* segment length,
10. Obtain the following segment midpoint location, using Eqs. (4) and (5) with the 1.5 ds segment length
11. Take *i* = *i*+1 and repeat steps 6 to10 until the final segment.
12. Go to step 4 and modify *du* and $\delta_{\max}$ until the predicted and calculated values are converged,
13. Calculate the effective width using Eqs. (13). Repeat the iteration from step 2 with the modified cross-section until the result converges.
14. Go to step 1 and increase the number of the segments to check the accuracy and convergence of the result.

1. Application of the Procedure

We studied a very simple and basic application of the procedure, which is a perfect centric axially loaded, perfectly straight, simply supported elastic beam-column (Fig. 7). The critical buckling load was determined to compare with classical methods.

For non-bifurcation buckling solutions, there are two equilibra, one in pre-buckling with a small displacement and the other in post-buckling with a large displacement. At the end of the iteration procedure, the equilibrium value of the midpoint displacement can be determined using the given axial load. For bifurcation buckling problems, a pre-buckling pattern was stabilized using a straight axis.

Appendix 1 presents the calculations of the first iteration and main properties of the beam-column. Fig. 8 presents the results of the first and subsequent iterations for a 3000 N axial load. For the subsequent iterations, the midpoint displacement was modified using a linear correction. Through several iterations, the midpoint deflection converged rapidly to zero at a given axial load. Fig. 9 shows the converged midpoint displacements as a function of the axial loads; the critical buckling load was ~4336 N with four segments.

Table 1. Critical Buckling Loads.

n	P_{cr} ($du \neq 0$, $dL \neq 0$)	P_{cr} ($du = 0$, $dL = 0$)
4	4336 N	4333 N
10	4446 N	4446 N
20	4445 N	4444 N
40	4443 N	4442 N
100	4440 N	4441 N
200	4440 N	4441 N

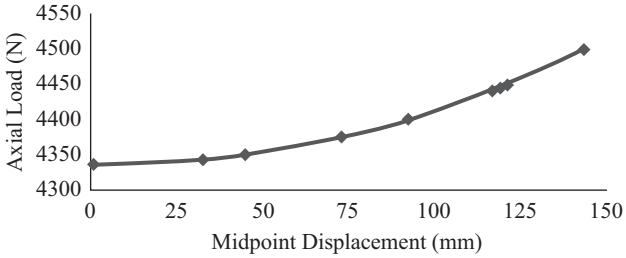

Fig. 9. Converged midpoint displacements against axial loads.

The accuracy was examined by increasing the number of segments, and the critical buckling load was 4440 N. If the secondary effect was neglected and the assumed shortening value was taken to be zero, the midpoint displacement will converge to approximately 4441 N, as the Euler buckling solution. Table 1 lists the critical buckling axial load values, P_{cr} considering the segment number and shortening value.

V. FRIGATE ANALYSIS

The applicability of the present method was tested by performing progressive collapse analysis on a large 1/3-scaled frigate model, which had been studied experimentally [2]. The properties of the frigate model were reported by Dow [2]. The welding residual stress was taken as one tenth of the yielding stress, as shown in Eq. (14) [4, 8]. The maximum initial deflection of the stiffened plates was calculated using the unsupported length, as shown in Eq. (15), where *a* is the distance between the frame spacing [4].

$$\sigma_R = 0.1\sigma_{yield} \tag{14}$$

$$\delta_{\max} = 0.0015a \tag{15}$$

The cross-section was divided into stiffened plates. In addition to the stiffened plate and plate members, there were corner members. The calculations were performed using the present method for a sagging situation.

When the ultimate strength was reached by performing the load shortening values into Smith's method [16], the location of the neutral axis was 1140 mm, whereas the curvature was 0.0013 l/m due to the predicted 9.74 MNm moment. Fig. 10 shows the moment-curvature diagram.

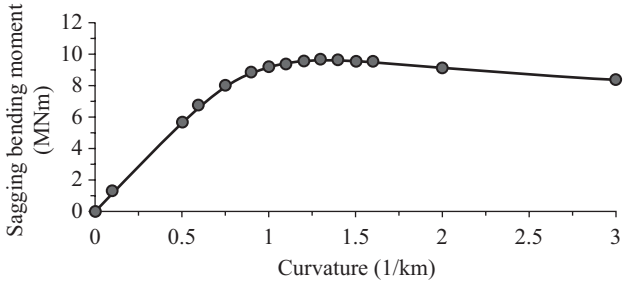

Fig. 10. Moment curvature diagram.

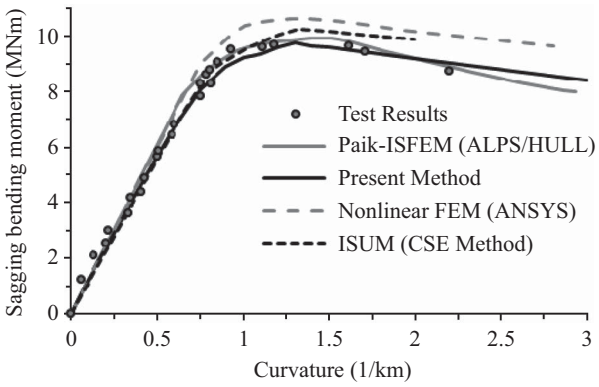

Fig. 11. Comparisons of the moment curvature diagrams.

The ultimate moment was measured to be 9.64 MNm [17]. The following data was obtained from the range of numerical and analytical methods reported elsewhere: 10.62 MNm by non-linear finite element analysis using ANSYS software [4, 6]; 9.83 MNm using the Idealized Structural Unit Method (ISUM) [4]; 9.94 MNm using the Intelligent Supersize Finite Element Method (ISFEM) using ALPS/HULL software; 5.59 MNm using the classical beam method [4]; 9.54 MNm reported by Chen using the ISUM [17]; 9.67 MNm reported by Dow using Smith's method including the shear and lateral load effects [17]; and 8.58 reported by Yao using the computer code, HULLST [17]. The proposed method yielded 9.74 MNm, which is close to the experimental results. Fig. 11 compares the moment curvature diagrams [4, 6].

VI. CONCLUSIONS

A new solution method for beam-columns on a bifurcation analysis was evaluated. The proposed method enabled the modeling of deflections with complex shapes and their application in the strength of stiffened plates and beam-columns. A geometrical representation of the curvature not only provides accuracy in deflection calculations but also has advantages in computation time. The rapid and accurate execution of progressive collapse analysis was realized.

A new solution was developed for individual ship structure members by considering the effects of the plate/stiffener interaction, initial deflections and welding residual stress using the curvature geometrically.

Using the developed method, progressive collapse analysis was performed using the solutions of the stiffened plate members. The proposed method produced reasonably accurate solutions with low modeling and computational times.

This application can be extended easily to non-bifurcation buckling analysis of beam-columns with initial deflection or lateral loads. In addition, strength calculations of stiffened plates can be performed by considering the effective width with reliable solutions.

APPENDIX 1

The main properties of the problem are given below. Only the half-length of the beam-column was considered due to the symmetric shape of the model. Total segment number is 4.

$$A = 120\ mm^2 \quad I = 1440\ mm^4 \quad L = 800\ mm$$

$$E = 200000\ N/mm^2 \quad F_x = 3000\ N$$

$$dL = (F_x L)/(EA) = 0.1\ mm$$

$$ds = (L - dL)/4 = 199.975\ mm$$

Calculations for the First segment:

$$du = 0.1\ mm \Rightarrow x_2 = 799.9\ mm \quad \delta_{\max} = 1\ mm \Rightarrow z_2 = 1\ mm$$

$$M_0 = F_x z_2 = 3000\ Nmm \quad r_{0,1} = (EI)/M_0 = 96000\ mm$$

$$d\theta_{0,1} = ds/r_{0,1} = -0.00208\ rad$$

$$\theta_1 = \theta_0 + d\theta_{0,1} = -0.00208\ rad$$

$$z_1 = 0.208\ mm \quad x_1 = 199.975\ mm$$

$$d\theta_{0,1'} = 1.5ds/r_{0,1} = -0.00312\ rad$$

$$z_{1'} = 0.469\ mm \quad x_{1'} = 299.962\ mm$$

Calculations for the Second segment:

$$M_{1'} = F_x z_{1'} = 1594.1\ Nmm$$

$$r_{1,2} = (EI)/M_{1'} = 180665.9\ mm$$

$$d\theta_{1,2} = ds/r_{1,2} = -0.001107\ rad$$

$$z_2 = 0.736\ mm \quad x_2 = 399.949\ mm$$

$$du = 2(L/2 - x_2) = 0.102\ mm$$

Initials for the second iteration:

$$du = 0.102\ mm \quad \delta_{\max} = 0.736\ mm$$

REFERENCES

1. Barsky, B. A. and DeRose, T. D., "Geometric continuity of parametric curves: three equivalent characterizations," *IEEE Computer Graphics & Applications*, Vol. 9, No. 6, pp. 60-68 (1989).
2. Dow, S. R., "Testing and analysis of a 1/3 scale welded steel frigate model," *Proceedings of the International Conference on Advances in Marine Structures*, pp. 749-773 (1991).
3. Faulkner, D., "A review of effective plating for use in the analysis of stiffened plating in bending and compression," *Journal of Ship Research*, Vol. 19, No. 1, pp. 1-17 (1975).
4. Huges, O. and Paik, J. K., *Ship Structural Analysis and Design*, The Society of Naval Architects and Marine Engineers (2010).
5. Paik, J., Branner, K., Choo, Y., Czujko, J., Fujikubo, M., Gordo, J., Parmentier, G., Iaccarino, R., O'neil, S., Pasqualino, I., Wang, D., Wang, X., and Zhang, S., "Ultimate strength," in: Jang C. D. and Hong, S. Y. (Eds.), *17th International Ship and Offshore Structures Congress*, Committee III.1, University of Seoul, Vol. 1, pp. 375-474 (2009).
6. Paik, J. K., Kim, D. K., Park, D. H., Kim, H. B., Mansour, A. E., and Caldwell, J. B., "Modified Paik-Mansour formula for ultimate strength calculations of ship hulls," *Ships and Offshore Structures*, Vol. 8, pp. 245-260 (2012).
7. Paik, J. K. and Thayamballi, A. K., *Ultimate Limit State Design of Steel-Plated Structures*, John Wiley & Sons (2003).
8. Paik, J. K., Thayamballi, A. K., and Kim, D. H., "An analytical method for the ultimate compressive strength and effective plating of stiffened panels," *Journal of Constructional Steel Research*, Vol. 49, pp. 43-68 (1999).
9. Paik, J. K., Thayamballi, A. K., Lee, S. K., and Kang, S. J., "A semi-analytical method for the elastic-plastic large deflection analysis of welded steel or aluminum plating under combined in-plane and lateral pressure loads," *Thin-Walled Structures*, Vol. 39, pp. 125-152 (2001).
10. Tayyar, G. T., *Determination of Ultimate Strength of Ship Hull Girder*, Ph.D. Thesis, Graduate School of Science Engineering and Technology, Istanbul Technical University, Istanbul, Turkey (2011). Available at: www.yok.gov.tr/en [Accessed 23.11.2012]. (in Turkish)
11. Tayyar, G. T., "A new analytical method with curvature based kinematic deflection curve theory," *International Journal of Ocean System Engineering*, Vol. 2, No. 3, pp. 195-199 (2012).
12. Tayyar, G. T. and Bayraktarkatal, E., "A new approximate method to evaluate the ultimate strength of ship hull girder," in: Rizzuto, E. and Soares, C. G. (Eds.), *Sustainable Maritime Transportation and Exploitation of Sea Resources*, Taylor & Francis, pp. 323-329 (2012).
13. Tayyar, G. T. and Bayraktarkatal, E., "Kinematic displacement theory of planar structures," *International Journal of Ocean System Engineering*, Vol. 2, No. 2, pp. 63-70 (2012).
14. Timoshenko, S., *Strength of Materials: Part I: Elementary Theory and Problems*, D. Van Nostrand Company (1948).
15. von Karman, T., Sechler, E. E., and Donnell, L. H., "The strength of thin plates in compression," *ASME Transactions*, Vol. 54, No. 5, pp. 53-57 (1932).
16. Yao, T., "Hull girder strength," *Marine Structures*, Vol. 16, pp. 1-13 (2003).
17. Yao, T., Astrup, O. C., Caridis, P., Chen, Y. N., Cho, S. R., Dow, R. S., Niho, O., and Rigo, P., "Ultimate hull girder strength, Special Task Committee VI.2," in: Ohtsubo, H. and Sumi, Y., (Eds.), *14th International Ship and Offshore Structures Congress*, Vol. 2, pp. 321-391 (2000).
18. Yu, W., *Cold-Formed Steel Design*, 3rd Edition, John Wiley & Sons (2000).